Received: 23 June 2019 | Revised: 10 September 2019 | Accepted: 22 September 2019

DOI: 10.1002/ardp.201900180

DPhG ARCH PHARM
Archiv der Pharmazie

FULL PAPER

Arginolipid: A membrane-active antifungal agent and its synergistic potential to combat drug resistance in clinical *Candida* isolates

Mrunal Patil[1] | Shashir Wanjare[2] | Vivek Borse[3] | Rohit Srivastava[3] | Preeti Mehta[2] | Pradeep Vavia[1]

[1]Department of Pharmaceutical Sciences and Technology, Institute of Chemical Technology, Mumbai, India

[2]Department of Microbiology, Seth G.S. Medical College and K.E.M. Hospital, Mumbai, India

[3]Department of Biosciences and Bioengineering, Indian Institute of Technology-Bombay (IIT-B), Mumbai, India

Correspondence
Prof. Pradeep R. Vavia, Department of Pharmaceutical Sciences and Technology, Institute of Chemical Technology, N.P. Marg, Matunga (E), Mumbai, Maharashtra 400019, India.
Email: pr.vavia@ictmumbai.co.in

Funding information
Department of Science and Technology, Ministry of Science and Technology, India, Grant/Award Number: Inspire Fellowship IF 130868

Abstract

Antifungal drug resistance exhibits a major clinical challenge for treating nosocomial fungal infections. To find a possible solution, we synthesized and studied the antifungal activities of three different arginolipids (N^{α}-acyl-arginine ethyl ester) against clinical drug-resistant isolates of *Candida*. The most active arginolipid, oleoyl arginine ethyl ester (OAEE) consisting of a long unsaturated hydrophobic chain, was tested for its mode of action, which revealed that it altered ergosterol biosynthesis and compromised the fungal cell membrane. Also, OAEE was found to exhibit synergistic interactions with fluconazole (FLU) or amphotericin B (AmB) against planktonic *Candida* cells, wherein it reduced the inhibitory concentrations of these drugs to their in vitro susceptible range. Studies conducted against the *C. tropicalis* biofilm revealed that the OAEE+AmB combination synergistically reduced the metabolic activity and hyphal density in biofilms, whereas OAEE+FLU was found to be additive against most cases. Finally, the evaluated selective toxicity of OAEE toward fungal cells over mammalian cells could establish it as an alternative treatment for combating drug-resistant *Candida* infections.

KEYWORDS
arginolipids, biofilms, *Candida*, drug resistance, membrane disruption, synergism

1 | INTRODUCTION

Incidences of fungal infections are expected to increase in the foreseeable future due to increased numbers of patients with immunodeficiency conditions.[1] Among existing fungal infections, *Candida* is the most common cause of opportunistic fungal disease and the fourth common cause of nosocomial bloodstream infections.[2] Over the decades, fluconazole (FLU) and amphotericin B (AmB) are being used as the drugs of choice in the management of candidiasis.[3] Though FLU has an excellent efficacy–toxicity profile, concomitant with its widespread use and owing to its fungistatic nature, clinical failures correlating with its elevated minimum inhibitory concentrations (MIC) have been reported in the past.[4] Conversely to AmB being the "gold standard"[5] for antifungal treatment, its use has been limited considering its nephrotoxic adverse effect and recent reports of resistance.[6,7] Additionally, the inhibitory concentrations of antifungal drugs have upsurged due to the unique ability of the *Candida* species to switch morphology and form biofilms. These biofilms are inherently tolerant to high antifungal doses and the host defense mechanism.[8] As a result, medical practitioners are provoked to use high doses of antifungal agents or opt for new drugs like echinocandins and second-generation triazoles,[9] but unfortunately, high cost, differential pharmacokinetics, unique predisposition of drug–drug interactions and the unusual toxicities associated with long-term therapy restricted their use.[10] Escalating toxic side effects and evolutionary pressure have incited an urgent need for developing new antifungal agents, preferentially, a

chemosensitizing agent, which augments the intracellular concentration of conventional antifungal drugs in the fungal cells, thereby making them susceptible even at low concentrations. One such category of the antifungal agent is cationic amino acid conjugated amphiphiles, that has gained popularity among researchers as next-generation therapeutic agents, primarily due to their notable antifungal activity.[11–13] As studied, the antifungal activity of these amphiphiles is a consequential outcome of their interaction with a negatively charged fungal cell membrane, which results in enhanced permeability.[14,15] These agents have advantages over other synthetic amphiphiles in the context of their ease of synthesis, low toxicity, biodegradability, and multifunctionality and are renewable sources of raw materials, which makes them a suitable choice for industrial scale-up.[16,17] Cationic amino acid-based amphiphiles especially arginine-based fatty acids (arginolipids) have been studied for their antifungal application in biomedical,[18] dermatological,[19] and food products[20,21]; however, till date, their proficiency to overcome drug resistance and their interaction with conventional antifungal drugs still remains unexplored. We, thereby, hypothesize that using arginolipid in combination with conventional antifungal drugs could enhance their potency, which may in turn aid in combating drug resistance. Hence, to study our hypotheses, we considered synthesizing three arginolipids (N^{α}-acyl-arginine ethyl ester), namely, decanoyl arginine ethyl ester (DAEE; Figure 1a), lauroyl arginine ethyl ester (LAEE, Figure 1b) and oleoyl arginine ethyl ester (OAEE; Figure 1c). These arginolipids were prepared by conjugating L-arginine ethyl ester with three different fatty acid chains. Arginine (Arg) as the head group was considered in the first place owing to its ability to delocalize the cationic charge within its guanidinium group and retain it regardless of being partially buried within fungal membrane protein.[22,23] Additionally, with a perspective of maintaining an optimum balance between polarity and hydrophobicity, three different fatty acids having a different chain length and the presence of unsaturation were considered for conjugating with Arg and the impact of their corresponding hydrophobicity on antifungal efficacy was evaluated.

The present study explores the antifungal activity of the synthesized arginolipids on clinical drug-resistant isolates of *Candida* and defining the mechanism of action of the most active arginolipid (OAEE). Furthermore, the interaction of OAEE with FLU and AmB separately was evaluated against clinical planktonic *Candida* cells and preformed *C. tropicalis* biofilms.

2 | RESULT AND DISCUSSION

2.1 | Synthesis

Arginolipids were synthesized and characterized using a previously published protocol by our research group.[24] These synthesized arginolipids consisted of a single L-arginine ethyl ester moiety conjugated to a lipophilic fatty acid. Fatty acids having a variable chain length and presence of the unsaturation state, namely, decanoic acid (C_{10}, saturated), lauric acid (C_{12}, saturated), and oleic acid (C_{18}, unsaturated), were used to yield DAEE, LAEE, and OAEE, respectively, and the effect of their resulting hydrophobicity on antifungal activity was evaluated.

2.2 | Antifungal activity of arginolipids

The MIC_{90} values of arginolipids tested against clinical drug-resistant *Candida albicans* and non-*albicans* isolates were found to be substantially diverse (Table S1). A possible reason for all arginolipids to exhibit low to moderate antifungal activity could be anticipated due to the presence of the cationic L-arginine head group. As studied previously,[25,26] the cationic guanidinium residues of Arg form stable electrostatic and hydrogen-bonding interactions with the anionic phosphodiester phospholipid content of fungal cell membranes, which results in pulling the phosphodiester phospholipid through the hydrophobic part of the membrane, simultaneously dragging along hydrogen-bonded water molecules to create a permeable toroidal pore, thus perturbing the fungal membrane. However, our studies suggest that the cationic group (polar group) alone is not responsible for the antifungal activity. The hydrophobicity imparted by the carbon chain length plays a major role in deciding the potency of antifungal activity. As observed, MIC_{90} of OAEE (15.25–62.5 μg/ml) were found to be comparatively lower than that of moderately active LAEE (31.25–250 μg/ml) and less-active DAEE (125–500 μg/ml). Apart from having a higher alkyl chain length (C_{18}), lower MIC of OAEE to some

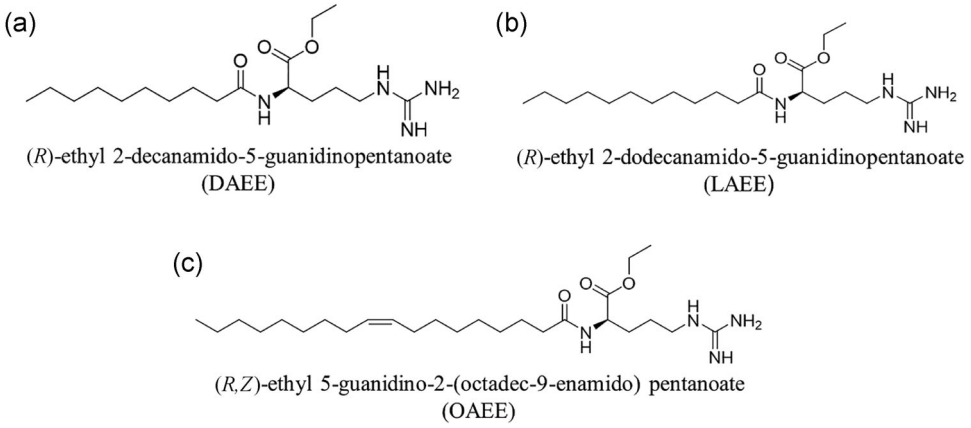

FIGURE 1 Chemical structures of the synthesized arginolipids

extent could be ascribed to the presence of kinking (fixed bend) within its hydrophobic carbon chain, which leads to formation of a different molecular conformation that occupies a greater cross-section due to increased motion freedom as it gets inserted into the fungal lipid bilayer, thereby, easily compromising membrane integrity.[27] On the contrary, LAEE showed comparatively low MIC than DAEE, possibly due to the presence of lauric acid (C_{12}), which is said to have the best balance between hydrophobic and hydrophilic groups, permitting it to reach sufficient concentrations to interact with acyl chains of membrane phospholipids.[24] Additionally, Paul and Jeffrey[28] showed that the critical micelle concentration (CMC) of an amphiphile is correlated with its antimicrobial property, as near CMC, an equilibrium is established between the lipid bilayer of cell membrane and a coexisting micellar pseudo phase in the aqueous medium, which results in dissolution of several components of the lipid bilayer into the formed micelles leading to obliteration of cell membrane integrity. Considering the given report, we investigated CMC values of arginolipids using the Nile Red encapsulation method (Supporting Information, Section S.3) and found them to be correlatable with their respective MIC. The low MIC exhibiting arginolipid, OAEE showed the lowest CMC (178 μM), followed by LAEE (261 μM) and DAEE (694 μM).

2.3 | Mechanism of action for OAEE

OAEE being the most active antifungal arginolipid, we speculate that it interacts with fungal cell membranes and might also contribute to altering the normal sterol biosynthetic pathway. To investigate our hypothesis, the sterol content of four clinical isolates subjected to different concentrations (MIC, MIC × 0.5, and MIC × 0.25) of OAEE was determined spectrometrically. A typical ultraviolet (UV) spectrum representing the sterol content of *C. albicans* SP360 upon treatment with different concentrations of OAEE is shown in Figure 2a (inset). The four-characteristic peak of spectra represents the presence of ergosterol and 24(28)-dehydroergosterol (24(28)-DHE). A dose-dependent decrease in height of the absorbance peaks with an increase in the concentration of OAEE indicated an alteration in the ergosterol biosynthesis pathway.[29,30] At MIC, a flat spectral curve was obtained, which signified the absence of detectable ergosterol in extracts. Similar results were observed among non-*albicans* species (Figure 2a). Hence, it can be interpreted that OAEE exhibits a dose-dependent effect on fungal sterol biosynthesis, which may conceivably alter membrane permeability.

To affirm the role of OAEE in membrane perturbation 3,3′-dipropylthiadicarbocyanine iodide ($DiSC_3(5)$), a membrane potential-dependent probe that rapidly accumulates into the bilayer of polarized cells causing its fluorescence to quench, was used. As observed from Figure 2b, addition of OAEE to *C. albicans* SP306 cell suspension resulted in rapid release of dye into the medium, causing an increase in fluorescence intensity. The response indicates that OAEE depolarizes the fungal membrane in a dose-dependent manner.

We then performed the propidium iodide (PI) dye exclusion assay to further support our hypothesis. PI is a membrane-impermeant dye that is generally excluded from viable cells unless their cell membrane is compromised. Upon entering the cell, PI intercalates itself within the nucleic acid and emits a fluorescence signal.[31] In the absence of OAEE (Figure 2c-i), the percentage of *C. albicans* SP306 cells with PI fluorescence was only 0.3%, indicating an intact cell membrane. After treatment with OAEE: MIC × 0.25, MIC × 0.5 and MIC, the PI fluorescence was found to be 20.15% (Figure 2c-iii), 70.6% (Figure 2c-iv) and 83.5% (Figure 2c-v), respectively, signifying dose-dependent membrane damage. Also, as observed at MIC, OAEE caused membrane disruption equivalent to that caused by 0.1% of Triton X-100 (Figure 2c-ii), which resulted in 86.9% PI-stained cells.

2.4 | Combination of OAEE with antifungal drugs against planktonic *Candida* cells

2.4.1 | Checkerboard and time-kill assay

The fractional inhibitory concentration index (FICI) calculated from the checkerboard assays is listed in Table 1. OAEE exhibited synergistic interaction with both AmB and FLU against all clinical *Candida* isolates. No indifferent or antagonist interactions were observed.

The time-kill curves (Figure 3) were studied to confirm synergistic interaction between OAEE and antifungal drugs. It was observed that the combinations (OAEE+FLU and OAEE+AmB) were relatively analogous in *C. albicans* and non-*albicans* isolates. Post 8 hr of incubation, OAEE+FLU resulted in >2 $\log_{10}$ CFU (colony-forming units)/ml decrease as compared to FLU alone in test isolates suggesting a synergistic interaction. Thereafter, at 12 hr, OAEE +FLU caused 3.029 and 3.134 $\log_{10}$ CFU/ml reduction as compared to FLU alone in *C. albicans* SP306 and *C. glabrata* BC199, respectively. A reduction of >3 $\log_{10}$ CFU/ml observed with OAEE+FLU combination indicated that OAEE converted fungistatic activity of FLU to fungicidal. It was worth noting that unlike OAEE+FLU, the combination of OAEE+AmB displayed synergistic activity in both the isolates precisely after 4 hr of incubation (>3 $\log_{10}$ CFU/ml). The OAEE+AmB combination caused 3.71 and 3.05 $\log_{10}$ CFU/ml reduction as compared to AmB alone in *C. albicans* SP306 and *C. glabrata* BC199, respectively. It can be inferred that the fungicidal activity of AmB was dramatically enhanced by the addition of OAEE.

2.4.2 | Molecular dynamic simulation (MDS) studies

Stability of interactions between OAEE+AmB and OAEE+FLU complexes was assessed by running their simulation trajectories and analyzing root mean square deviation (RMSD) and root mean square fluctuation (RMSF) parameters. It was observed that OAEE +AmB and OAEE+FLU complexes exhibited a hydrogen-bonding interaction along with hydrophobic and the van der Waals interactions. As analyzed, the OAEE+AmB complex showed two hydrogen-bonding interactions (Figure 4a): (a) between AmB's carbonyl oxygen (C═O) of the carboxylic acid with amine functionality (–NH–) of the amide group of OAEE, (b) between AmB's hydroxyl group (–OH–) of carboxylic acid and amine functionality (–NH_2–) of guanidine in OAEE. In the case of OAEE

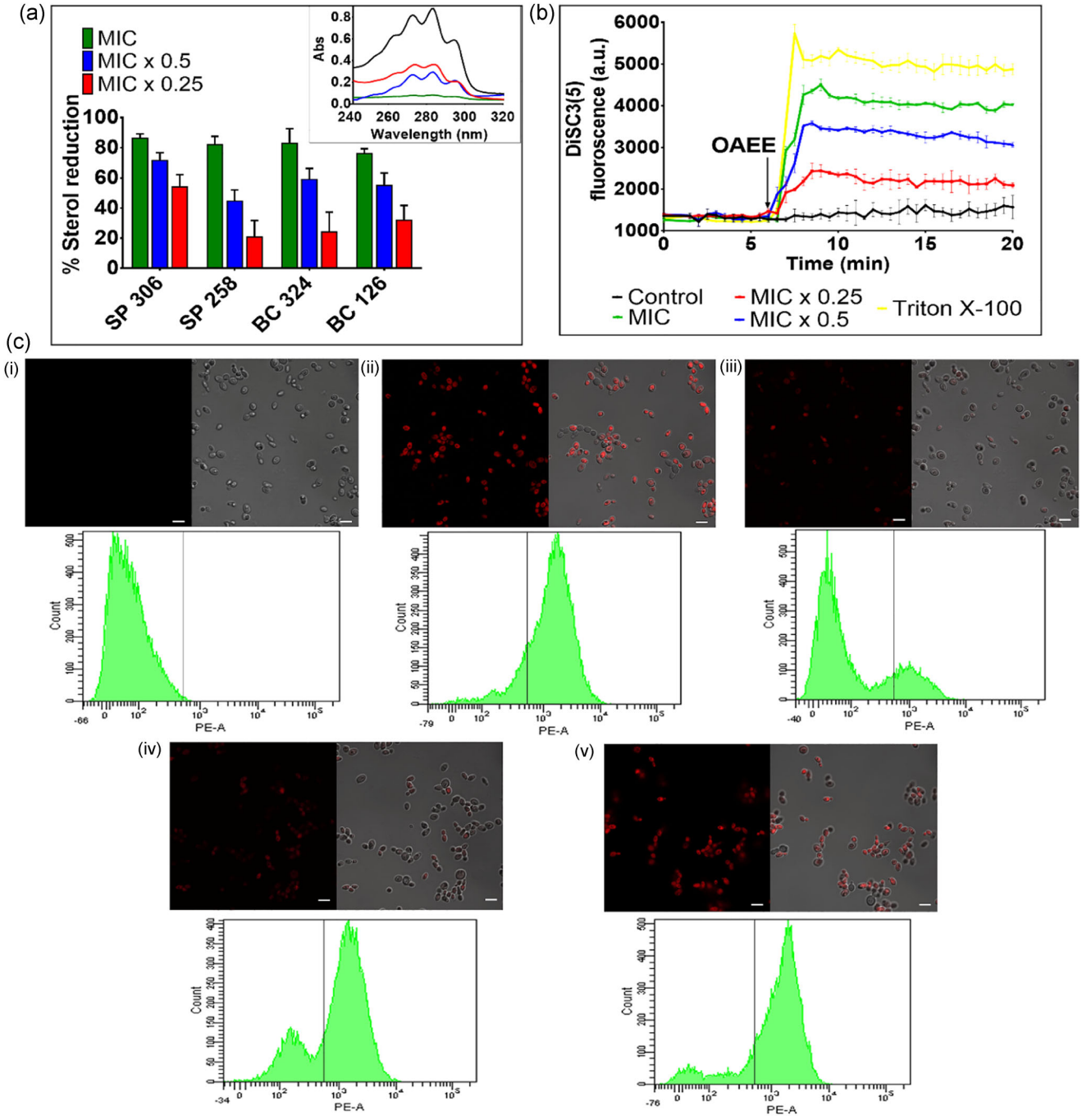

FIGURE 2 (a) Bar graph representing percentage reduction in ergosterol content of treated samples in comparison with control cells (physiological saline solution treated) expressed as mean ± standard deviation. The inset figure represents a typical UV spectrophotometrically obtained sterol profile of *Candida albicans* SP306. (b) Depolarization of *C. albicans* SP306 cell membrane using $DiSC_3(5)$ assay. (c) Flow cytometric graph and confocal laser-scanning microscopy image representing membrane permeabilization of *C. albicans* SP306 using the propidium iodide dye exclusion assay for (i) untreated cells, (ii) 0.1% Triton X-100, (iii) OAEE–MIC × 0.25 (7.81 μg/ml), (iv) OAEE–MIC × 0.5 (15.62 μg/ml), and (v) OAEE–MIC (31.25 μg/ml) treated cells. For flow cytometry, the data was collected from 25,000 to 35,000 cells. The scale bar = 5 μm. $DISC_3(5)$, 3,3′-dipropylthiadicarbo-cyanine iodide; MIC, minimum inhibitory concentrations; OAEE, oleoyl arginine ethyl ester; UV, ultraviolet

+FLU, hydrogen-bonding interaction was seen between the nitrogen (–N–) of the triazole ring with amine functionality ($–NH_2–$) of guanidine in OAEE (Figure 4b). Also, as analyzed, the average RMSD values for OAEE+AmB and OAEE+FLU complex were found to be 5.05 and 6.64 Å, respectively, whereas the average RMSF values for OAEE+AmB and OAEE+FLU complex were found to be 7.32 and 8.33 Å, respectively. As evident, these values were considerably lower, which indicated that the complexes so formed are stable.[32] Interestingly, though an equilibration stage of both the complexes was achieved smoothly within 2 ns, fluctuations were more evident

TABLE 1 Minimum inhibitory concentrations and in vitro interactions between OAEE and antifungal drugs (FLU and AmB) against drug-resistant clinical isolates of *Candida*[a]

Species	Isolate number	MIC_{90} of antifungal agents expressed in μg/ml								
		MIC tested alone			MIC in combination (OAEE + FLU)			MIC in combination (OAEE + AmB)		
		FLU	AmB	OAEE	OAEE	FLU	FICI	OAEE	AmB	FICI
Candida *albicans*	SP237	128	1	31.25	3.90	16	0.25 (S)	3.90	0.25	0.37 (S)
	SP190	64	2	62.5	7.81	2	0.31 (S)	3.90	0.25	0.12 (S)
	SP306	128	2	31.25	7.81	8	0.37 (S)	3.90	0.25	0.18 (S)
	M180	16	4	62.5	3.90	2	0.25 (S)	7.81	0.5	0.25 (S)
	BC372	64	1	31.25	1.95	8	0.18 (S)	1.95	0.12	0.18 (S)
Candida tropicalis	BC321	32	2	31.25	1.95	2	0.12 (S)	3.90	0.12	0.12 (S)
	SP258	64	0.25	62.5	15.62	2	0.18 (S)	15.62	0.01	0.31 (S)
	SP411	64	2	31.25	1.95	16	0.28 (S)	1.95	0.25	0.18 (S)
	M206	64	0.5	62.5	15.62	8	0.37 (S)	7.81	0.06	0.25 (S)
	M280	64	4	15.25	3.90	4	0.31 (S)	1.93	0.25	0.18 (S)
Candida haemulonii	BC379	32	8	31.25	15.62	2	0.31 (S)	7.81	1	0.37 (S)
	BC324	64	8	62.5	15.62	2	0.31 (S)	7.81	1	0.2 (S)
	BC405	64	8	62.5	15.62	8	0.31 (S)	3.90	1	0.18 (S)
	BC380	64	8	62.5	15.62	4	0.37 (S)	7.81	0.5	0.18 (S)
Candida glabrata	BC194I	128	1	62.5	31.25	16	0.37 (S)	15.62	0.12	0.37 (S)
	BC194II	128	1	62.5	7.81	16	0.25 (S)	15.62	0.12	0.37 (S)
	BC460	64	4	31.25	3.90	4	0.18 (S)	7.81	0.5	0.25 (S)
	BC426	64	2	62.5	15.62	8	0.37 (S)	7.81	0.5	0.37 (S)
	BC126	128	1	62.5	15.62	16	0.18 (S)	7.81	0.12	0.25 (S)
	BC199	128	4	62.5	7.81	16	0.25 (S)	7.81	0.5	0.25 (S)
	BC571	64	1	31.25	3.90	4	0.18 (S)	7.81	0.12	0.25 (S)

Abbreviations: AmB, amphotericin B; FICI, fractional inhibitory concentration index; FLU, fluconazole; MIC, minimum inhibitory concentrations; OAEE, oleoyl arginine ethyl ester; S, synergism.

[a]MIC represented are an average of at least two independent experiments and each experiment was performed in triplicate.

in OAEE+FLU as compared to OAEE+AmB complex (Figure 4d), thus suggesting that the OAEE+AmB complex had better stability in comparison with OAEE+FLU. Hence, it could be inferred that the stable hydrogen bond and van der Waals interactions between OAEE and antifungal could be one of the possible reasons for their enhanced antifungal effect in combination.

2.4.3 | Atomic force microscopy (AFM)

Morphological damage was assessed by comparing the diameter versus height plot of control and treated cells. Roughness expressed as the root mean square (RMS) value was analyzed using AFM. Control *C. albicans* SP306 cells (Figure 5a) displayed a smooth and uniform surface

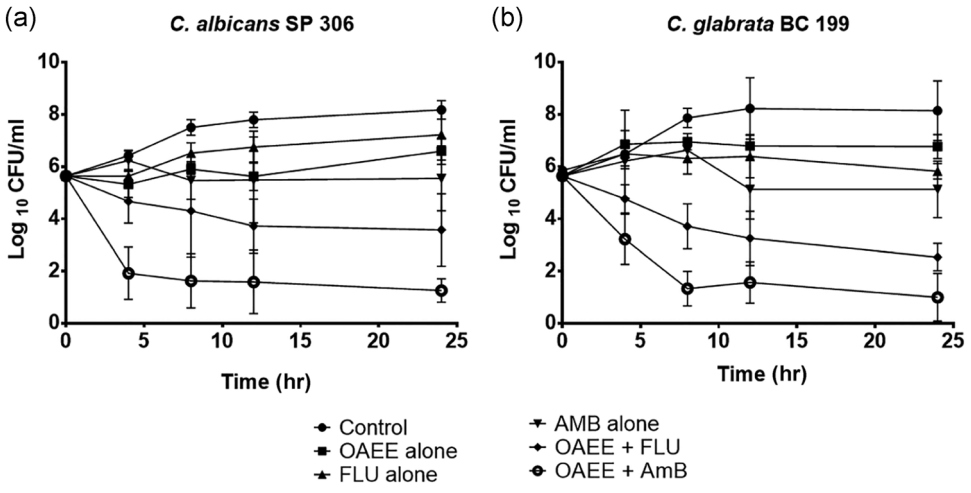

FIGURE 3 Time-kill curves of (a) *Candida albicans* SP306 and (b) *C. glabrata* BC199 isolate obtained after treating with OAEE, AmB, and FLU alone and in combination. The concentrations tested against *C. albicans* SP306 isolate were FLU (64 μg/ml), AmB (1 μg/ml), OAEE (15.62 μg/ml), and their respective combinations. For *C. glabrata* BC199 the concentration tested were FLU (64 μg/ml), AmB (2 μg/ml), OAEE (31.25 μg/ml), and their respective combinations. The experiments were performed three times. Data were expressed as mean ± standard deviation. AmB, amphotericin B; CFU, colony-forming units; FLU, fluconazole; OAEE, oleoyl arginine ethyl ester

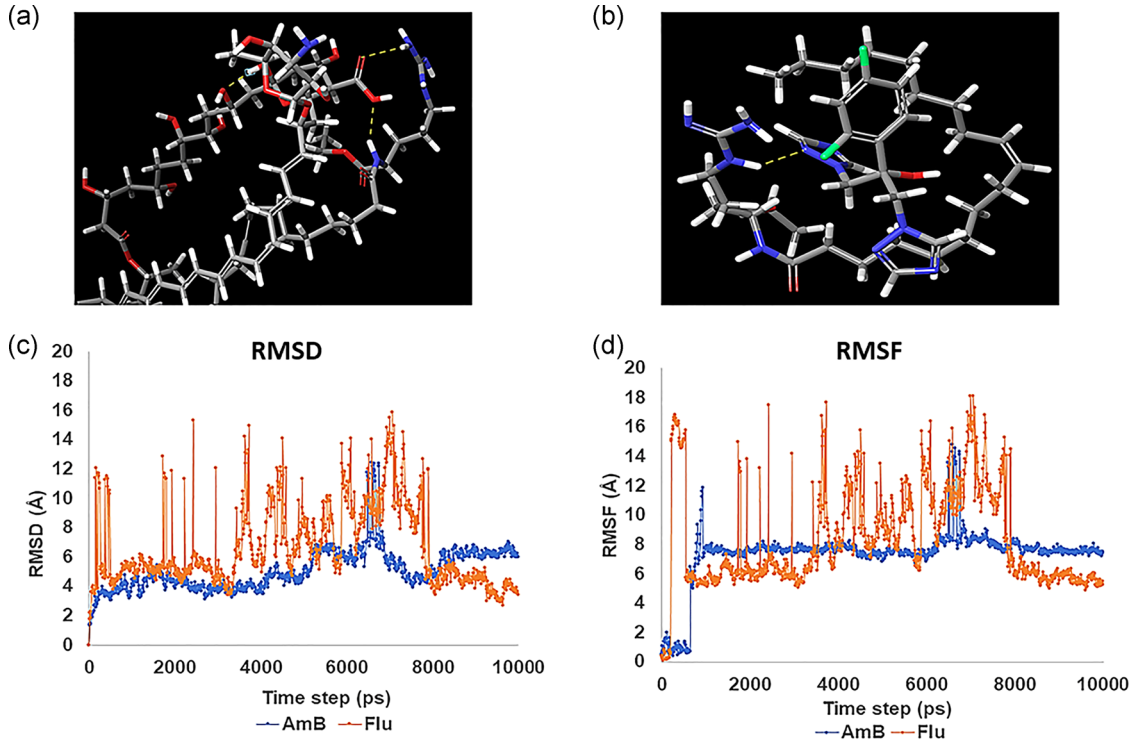

FIGURE 4 (a) Hydrogen-bonding interactions (yellow line) between OAEE–AmB. (b) Hydrogen-bonding interactions (yellow line) between OAEE+FLU. (c) RMSD plot and (d) RMSF plot of OAEE+AmB and OAEE+FLU complexes. AmB, amphotericin B; FLU, fluconazole; OAEE, oleoyl arginine ethyl ester; RMSD, root mean square deviation

(RMS = 228.7 nm). Cells exposed to a subinhibitory concentration of OAEE (Figure 5b), FLU (Figure 5c), and AmB (Figure 5d) exhibited significant ($p < 0.05$) increase in surface roughness RMS = 300.6, 272.5, and 335.03 nm, respectively, which suggested minor to moderate surface deformation (wrinkle formation). However, cells exposed to OAEE+FLU (Figure 5e) and OAEE+AmB (Figure 5f), displayed an enormous ($p < 0.01$) increase in surface roughness RMS = 595.2 and 423.1 nm, respectively as compared to control, signifying complete deformation of surface integrity. These deformations are the consensual outcome of the collapsed cell membranes due to leakage of internal cell content.

2.5 | Activity of OAEE and its combinations on preformed *C. tropicalis* biofilm

C. tropicalis has been recognized as a biofilm producer, surpassing *C. albicans*.[33] The ability of *C. tropicalis* to survive in high salt concentration and form a low-carbohydrate-containing extracellular matrix (ECM) makes them more resistant toward detachment from the surface.[34] Thus, OAEE and its combination with antifungal agents were investigated on the preformed biofilm of drug-resistant clinical isolates of *C. tropicalis*.

2.5.1 | Minimal biofilm eradication concentration (MBEC)

The preformed biofilms of clinical *C. tropicalis* isolates were found to be resistant to FLU and AmB (Table 2). A significant eradication of biofilm was obtained with FLU, only at high concentration, that is, >512 μg/ml and that for AmB was found to be 4–16 μg/ml. The MBEC value of OAEE ranged between 250 and 1,000 μg/ml.

2.5.2 | Checkerboard assay

The combination of OAEE+FLU exhibited synergistic interactions only among three out of five preformed biofilms of *C. tropicalis* isolates. It was worth noting that despite the synergism, the combinatorial MIC of FLU (MIC of FLU obtained in combination study with OAEE) ranged between 32 and 128 μg/ml which, as per CLSI M27-A2 guidelines,[35] falls under non-susceptible (i.e dose-depended/resistant) concentration.[35] Therefore, the OAEE+FLU combination failed to reduce the MIC of FLU to a susceptible range. Conversely, OAEE+AmB exhibited a synergistic interaction among all tested isolates and the combinatorial MIC of AmB was found to be <1 μg/ml (susceptible range), excepting for *C. tropicalis* M280 (4 μg/ml).

2.5.3 | Atomic force microscopy

Morphological changes within the treated *C. tropicalis* M206 biofilms were analyzed by comparing their resulting roughness (RMS) and cellular build-up (maximum height, h_{max}) against that of control biofilms. The three-dimensional (3D) AFM topographical images of control biofilms (Figure 6a) revealed a dense and heterogeneous network of yeast, pseudo-hyphae, and hyphae having RMS = 564.9 nm and h_{max} = 6.786 μm. Biofilms treated with a subinhibitory concentration of OAEE (RMS = 609.7 nm and h_{max} = 6.564 μm) and

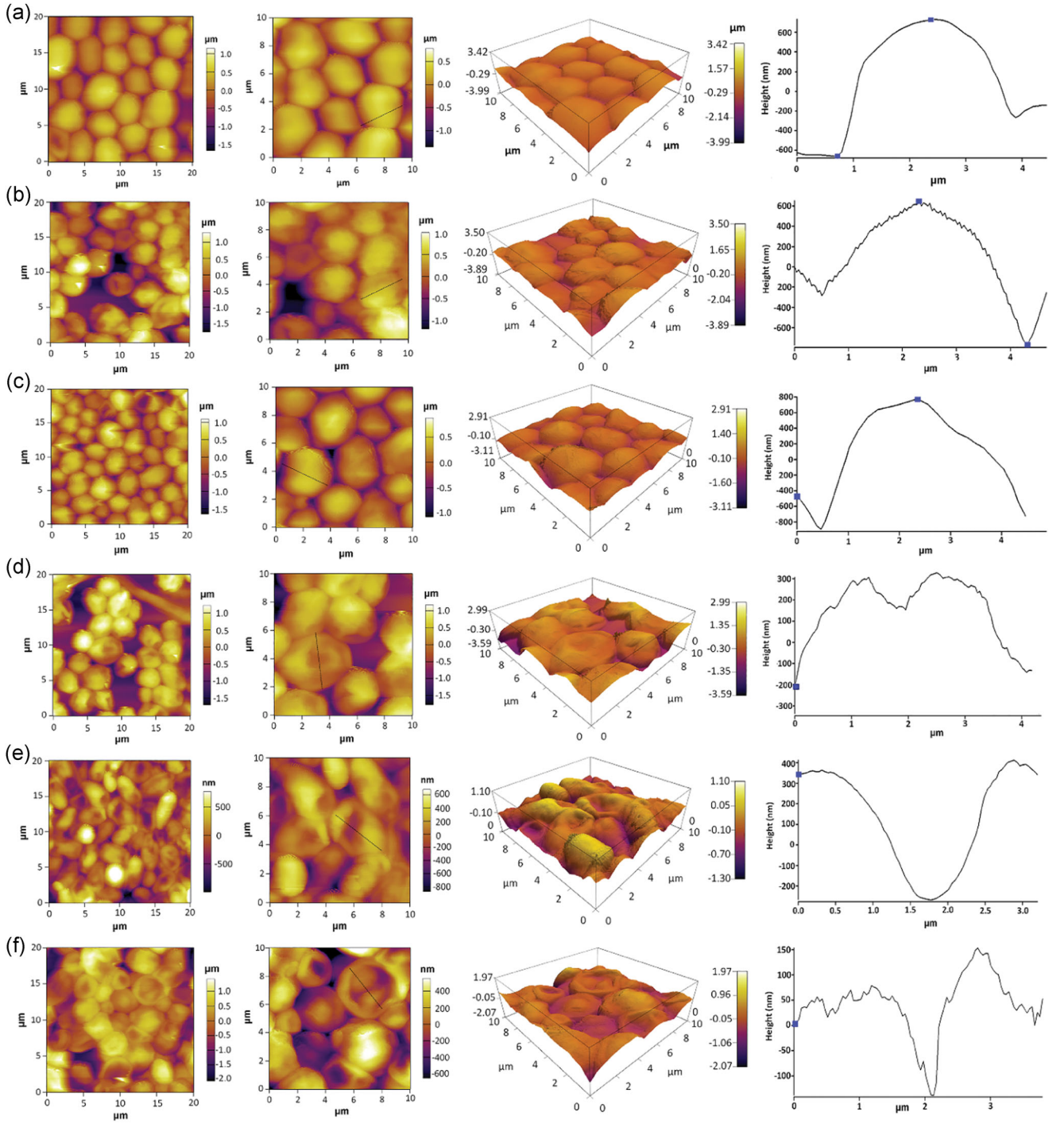

FIGURE 5 AFM tapping mode images of *Candida albicans* SP306 upon treatment with (a) physiological saline (control), (b) OAEE (15.62 µg/ml), (c) FLU (64 µg/ml), (d) AmB (1 µg/ml), (e) OAEE+FLU (15.62 + 64 µg/ml) combination, and (f) OAEE+AmB (15.62 + 1 µg/ml) combination. The data exhibited consist of two- and three-dimensional images along with the height versus diameter curve of the marked cell (black dotted lines). AFM, Atomic force microscopy; AmB, amphotericin B; FLU, fluconazole; OAEE, oleoyl arginine ethyl ester

FLU (RMS = 591.7 nm and h_{max} = 6.507 µm) showed few surface irregularities but no significant reduction in their cellular densities was observed (Figure 6b and Figure 6c, respectively). Interestingly, a significant ($p < 0.05$) decrease in the maximum height of biofilms was observed (RMS = 400.6 nm, h_{max} = 5.932 µm) with a subinhibitory concentration of AmB (Figure 6d), hence, signifying minor sensitization to the subjected dose. Biofilms subjected to a combination of OAEE + FLU (Figure 6e) and OAEE+AMB (Figure 6f) exhibited a significant ($p < 0.01$) increase in surface roughness (RMS = 712.0 and 651.7 nm, respectively) and a drastic reduction ($p < 0.01$) in maximum height (h_{max} = 3.406 and 3.120 µm, respectively) was observed. Though both combinations exhibited a flattened and furrowed surface; it was OAEE–AMB that distinctively reduced cell density as compared to OAEE+FLU (visually confirmed).

TABLE 2 Minimum biofilm eradication concentration ($MBEC_{50}$) and *in vitro* interaction between OAEE and antifungal drugs against preformed biofilms of *Candida tropicalis*

Candida tropicalis species	MIC_{50} of antifungal agents expressed in μg/ml								
	$MBEC_{50}$ tested alone			$MBEC_{50}$ in combination (OAEE + FLU)			$MBEC_{50}$ in combination (OAEE + AmB)		
	OAEE	FLU	AmB	OAEE	FLU	FICI	OAEE	AmB	FICI
BC321	250	128	8	31.25	64	0.37 (S)	62.5	1	0.37 (S)
SP258	1,000	256	4	125	128	0.62 (I)	250	0.5	0.37 (S)
SP411	500	512	8	125	256	0.75 (I)	62.5	1	0.25 (S)
M206	250	256	4	62.5	64	0.5 (S)	62.5	0.25	0.31 (S)
M280	500	512	16	62.5	128	0.25 (S)	62.5	4	0.37 (S)

Abbreviations: AmB, amphotericin B; FICI, fractional inhibitory concentration index; FLU, fluconazole; I, indifference; MIC, minimum inhibitory concentrations; OAEE, oleoyl arginine ethyl ester; S, synergism.

2.6 | Cytotoxicity studies

To justify the selectivity of the OAEE toward fungal cells in comparison to mammalian cells, we evaluated its cytotoxicity, against HepG2 cells, an immortalized human liver hepatocellular carcinoma cell line, and HEK 293 cells, an immortalized human embryonic kidney cell line. It was observed that the GI_{50} value of OAEE against HEK 293 and Hep2G (Figure S14) was found to be 44.3 and >80 μg/ml, whereas, LC_{50} values for both the cell lines were found to be >80 μg/ml, which is approximately more than 1.5 to 2-fold higher than the MIC values of OAEE obtained against planktonic clinical isolates of *Candida* (15.25–62.5 μg/ml). Presumably, this effect could be attributed to the fundamental differences between the plasma membrane of the mammalian and fungal cells. The fungal cell plasma membrane contains ergosterol, which has a higher percentage of negatively charged lipids such as phosphatidylinositol, which are known to interact with antifungal cationic molecules.[11] Hence, it can be said that OAEE was selectively toxic toward fungal cells over mammalian cells due to its interaction with ergosterol containing fungal cells than cholesterol containing mammalian cells.

3 | CONCLUSION

As evident from our experimental work, OAEE exhibited superior antifungal activity not only due to its cationic head group but also due to the presence of a higher alkyl chain (lipophilicity) consisting of a structural kink. However, the role of structural kinking in antifungal activity needs further investigation. OAEE compromised the fungal cell membrane by affecting its content. This mechanism indeed was responsible for OAEE exhibiting synergistic interaction with tested antifungal drugs. Studies conducted against clinical drug-resistant planktonic *Candida* isolates and the preformed *C. tropicalis* biofilm suggested that OAEE fluidizes the fungal cell membrane, permitting easy entry of antifungal agents, thereby potentially reducing the MIC of AmB and transforming the fungistatic nature of FLU to fungicidal. These results were supported by atomic force microscopy analysis, which revealed that OAEE and antifungal drug combination together caused cellular content leakage in both planktonic *Candida* cells and biofilms. The combination of OAEE+AmB was more effective in reducing biofilm density. Additionally, our studies revealed that OAEE is less cytotoxic and could be considered for its use to combat drug resistance. However, in the case of antibiofilms therapy, the application of OAEE could only be extended to implantology as its dose in combination was still found to be comparatively high.

Briefly, considering the amphiphilic nature of OAEE, we intend to explore its potential role in entrapping and formulating antifungal drugs into pharmaceutical emulsions in the near future. Also, we presume that the OAEE-assisted polymeric or lipidic pharmaceutical formulation could further minimize the cytotoxicity profile of OAEE. Thus, it is expected that this unique combination involving arginolipids and antifungal agents could serve an alternative to replace conventional monotherapies and would widen the potential treatment choice against drug-resistant *Candida* species.

4 | EXPERIMENTAL

4.1 | General

Roswell Park Memorial Institute medium (RPMI-1640; with L-glutamine, 2% glucose with 0.165 mol/l 3-morpholinopropanesulfonic acid, pH 7.0 ± 0.1), $DiSC_3(5)$, resazurin sodium salt, PI, 2,3-bis(2-methoxy-4-nitro-5-sulfophenyl)-2*H*-tetrazolium-5-carboxanilide salt (XTT), FLU, and AmB was purchased from Sigma-Aldrich (St. Louis, MO). Sabouraud dextrose agar (SDA) was purchased from Hi-Media (India). All other inorganic chemicals were purchased from Merck (India). Water used was obtained from the Milli-Q system, Millipore Corporation. Clinical isolates of *Candida* were obtained from routine specimens taken from in-house patients of K.E.M. Hospital, Mumbai. These specimens were collected, isolated, identified, and coded (according to their source of isolation, viz., BC: blood culture, SP: sputum, and M: miscellaneous were used as a prefix) at the Department of Microbiology, K.E.M Hospital and G. S. Seth Medical College, Mumbai (ethical approval no. EC/OA-60/2014). Isolates used in the present study were drug-resistant against FLU/AmB or both. Drug resistance was screened using the CLSI M27-A2 microbroth dilution protocol.[35] The list of drug-resistant isolates with their respective MIC is given in Table 1.

The InChI codes of the investigated compounds together with the biological activity data are provided as Supporting Information.

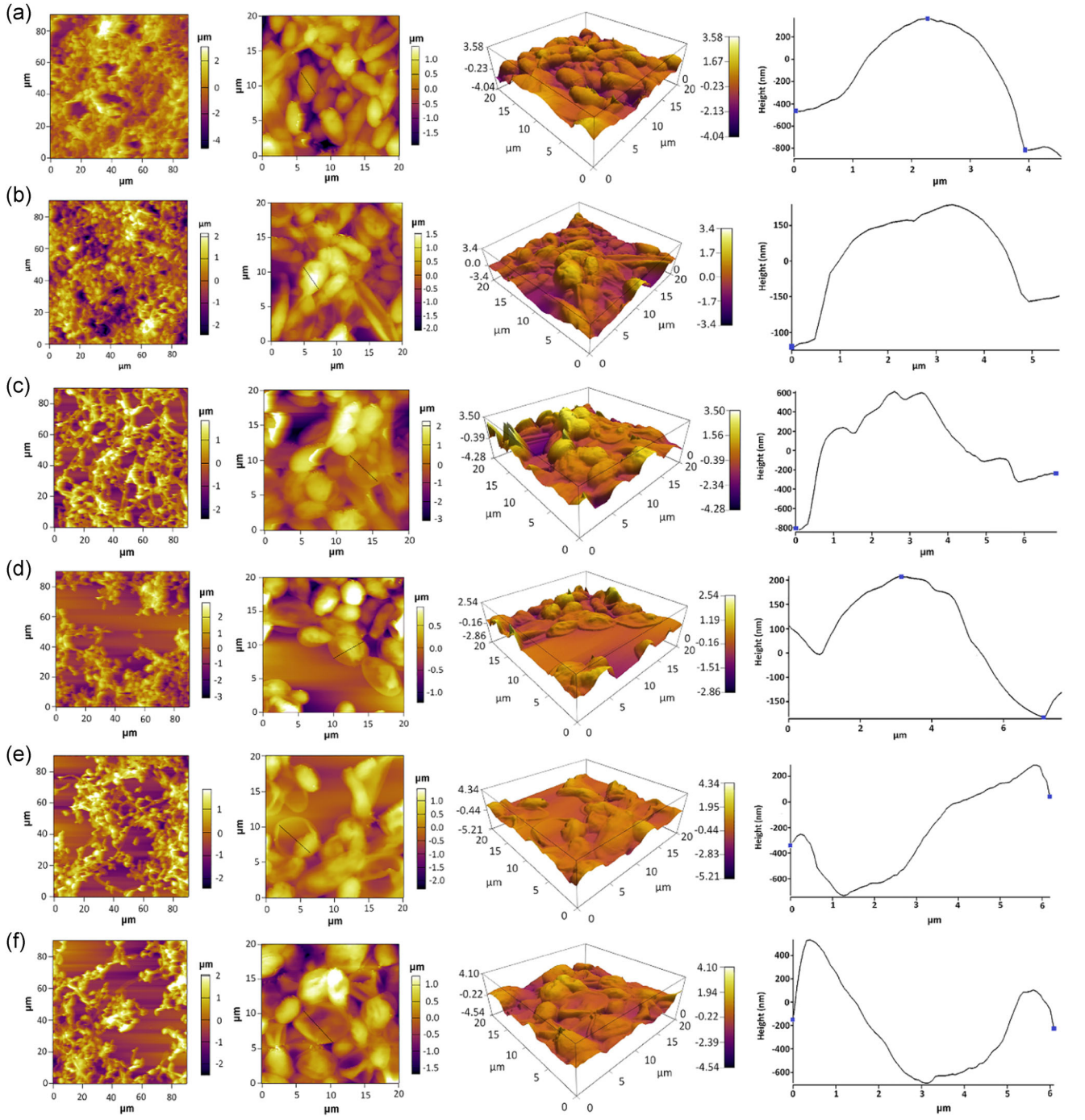

FIGURE 6 AFM tapping mode images of *Candida tropicalis* M206 biofilms upon treatment with (a) physiological saline (control), (b) OAEE (125 µg/ml), (c) FLU (128 µg/ml), (d) AmB (2 µg/ml), (e) OAEE+FLU (125 + 128 µg/ml) combination, and (f) OAEE+AmB (125 + 2 µg/ml) combination. The data exhibited consist of two- and three-dimensional images along with height versus diameter curve of the cell (black dotted lines)

4.2 | Synthesis

The syntheses of arginolipids, namely DAEE, LAEE, and OAEE, were carried out using the Schotten Baumann reaction protocol previously published by our research group.[24] The synthesized arginolipids were characterized using spectrometric analytical methods (Supporting Information, Section S.1) and their CMC was determined using the Nile Red encapsulation method (Supporting Information, Section S.2).

4.3 | Antifungal activity of arginolipids

The MIC_{90} of synthesized arginolipids was determined against drug-resistant clinical isolates of *Candida* using the CLSI M27-A2 broth microdilution protocol.[35] Briefly, the primary stock solution of synthesized arginolipids was appropriately diluted to two-fold strength (<1% dimethyl sulfoxide [DMSO]) of the desired concentrations (7.812–1000 µg/ml) using RPMI-1640 medium. An aliquot

(100 µl) of prepared dilution was added to wells of a sterile, flat-bottomed 96-well microtitration plate (Hi-Media), separately followed by the addition of 100 µl of a freshly prepared mid-exponential phase *Candida* cell suspension (2.5×10^3 CFU/ml). Media and growth control were included in all plates, and they were incubated in a shaker incubator operated at 200 rpm at 35°C for 24 hr. Post incubation, 20 µl of resazurin solution (0.015%w/v) was added to each well followed by incubation at 35°C for 30 min. The MIC_{90} values were then determined by measuring fluorescence (emission 590 nm and excitation 560 nm) using a multimode microplate reader (BioTek Synergy™ H1).[36,37]

4.4 | Mechanism of action for OAEE

4.4.1 | Sterol quantification method (SQM)

OAEE being the most active arginolipid, its sensitivity towards sterol biosynthesis process was determined using the SQM protocol reported by Arthington-Skaggs et al.[29] This method gives an absolute in vitro measurement of steady-state amounts of membrane ergosterol following the addition of various concentrations of OAEE, that is, MIC, MIC × 0.5 and MIC × 0.25 to cell suspension of *Candida* isolates. Briefly, 24 hr incubated OAEE and physiological saline solution treated (control) cells were harvested (3,000*g*, 1 min at 4°C), weighed and digested with 25%w/v ethanolic potassium hydroxide solution at 85°C for 1 hr. Post digestion, the non-saponifiable lipid content was extracted by the addition of a *n*-heptane/sterile water (3:1) mixture. The *n*-heptane layer was then separated and analyzed using a UV/Visible spectrophotometer (Jasco) for the presence of ergosterol and the late sterol intermediate 24(28)-DHE. The ergosterol content was calculated as a percentage of the wet weight of cells using the following equations:

$$\%\text{Ergosterol} + \%24(28)\text{-DHE} = [(A281.5/290) \times F] / \text{pellet weight},$$

$$\%24(28)\text{-DHE} = [(A230/518) \times F]/\text{pellet weight},$$

$$\%\text{Ergosterol} = [\%\text{Ergosterol} + \%24(28)\text{-DHE}] - \%24(28)\text{-DHE},$$

where *F* is the factor for dilution in ethanol and 290 and 518 are the *E*-values (%/cm) determined for ergosterol and 24(28)-DHE, respectively.

4.4.2 | Depolarization of fungal cell membrane

C. albicans SP306 cell suspension (1×10^7 cells/ml) was prepared in 5 mM 4-(2-hydroxyethyl)-1-piperazineethanesulfonic acid (HEPES), 5 mM glucose and 5 mM KCl solution (1:1:1). To the prepared cell suspension, $DiSC_3(5)$ dye was added to achieve a 2-µM final concentration. An aliquot (190 µl) of suspension containing dye was then transferred to a black 96-well plate and preincubated for 20 min. The quenched fluorescence (due uptake of dye in bilayers of the cell) was measured at excitation, 622 nm and emission, 670 nm, using a multimode microplate reader. Furthermore, 10 µl of OAEE (final concentration equivalent to its MIC, MIC × 0.25, and MIC × 0.5) was added to wells, separately and the fluorescence intensity was measured every minute for 30 seconds. Untreated and Triton X-100 (0.1%)-treated cells served as negative and positive controls.

4.4.3 | PI dye exclusion assay

An aliquot (100 µl) of OAEE concentration equivalent to its MIC, MIC × 0.25, and MIC × 0.5 was added to 900 µl of *C. albicans* SP306 cell suspension (1×10^7 cells/ml) prepared in 5 mM HEPES and 5 mM glucose (pH 7.4) and incubated at 35°C for 60 min. Cells were harvested and resuspended in 900 ml of 5 mM HEPES solution. An aliquot of 100 µl of PI solution (1 mg/ml) was added to resuspended cells and incubated for another 15 min at room temperature in the dark. Data was collected using a flow cytometer instrument (Beckman Coulter XL-MCL) equipped with a 15 mV argon laser from 25,000 to 35,000 cells at excitation of 488 nm and emission of 614/650 nm.[38] Data analysis was performed using FlowJo 8.7 software. Untreated cells and 0.1% Triton X-100 (membrane lytic agent)-[39] treated cells served as the negative and positive control, respectively. The cells were photographed using a confocal laser-scanning microscope (Zeiss LSM780; Germany) and images were processed on zen black and zen blue software.

4.5 | Combination of OAEE with antifungal drugs against planktonic *Candida* cells

4.5.1 | Checkerboard assay

The in vitro interaction of OAEE with FLU and AmB, separately against clinical drug-resistant isolates of *Candida* was tested using a two-dimensional (2D) broth microdilution checkerboard technique. A four-fold strength of the desired antifungal drugs and OAEE test concentrations were prepared in RPMI-1640 (<1%v/v DMSO). An aliquot (50 µl) of each antifungal drug (FLU/AmB) concentration was added to columns 1 to 8 of 96-well plate, separately followed by addition of 50 µl of each concentration of OAEE to rows A to H. Freshly prepared *Candida* cell suspension (2.5×10^3 CFU/ml) was added to each well excluding the media control wells. Plates were incubated at 35°C for 24 hr. The MIC_{90} values were determined by using the resazurin assay. The data obtained from the spectrometric method were analyzed nonparametrically with the Loewe additivity (LA) model. FICI was calculated using the following equation.

$$\text{FICI} = (C_A^{comb}/MIC_A^{alone}) + (C_B^{comb}/MIC_B^{alone}),$$

where C_A^{comb} and C_B^{comb} are the concentrations of drugs A and B at isoeffective combinations respectively. MIC_A^{alone} and MIC_B^{alone} are the MIC values of drugs A and B when acting alone. FICI of ≤0.5 represented synergy, values between >0.5 and 4 represented indifference, and values ≥4 represented antagonism.[40]

4.5.2 | Time-kill assay

Time-kill curves were studied to confirm synergism and fungicidal activity of combinations. Time-kill assay of OAEE in the presence and absence of FLU/AmB was evaluated against one of *C. albicans* (SP306), and the one of *C. non-albicans* (*C. glabrata* BC199) species. *Candida* inoculums (5×10^5 CFU/ml) were prepared in RPMI-1640 medium and subjected to OAEE concentration equivalent to its (0.5 × MIC) alone, FLU/AmB (0.5 × MIC) alone and combinations, separately. DMSO comprised <1% of the total test volume. These cultures were then incubated at 35°C with continuous shaking at 200 rpm. An aliquot of 100 µl was removed at predetermined time intervals (0, 4, 8, 12, and 24 hr), harvested, washed three times with sterile physiological saline (PS) and serially diluted in RPMI-1640 medium. An aliquot of 20 µl from each dilution was spread onto the SDA plates and incubated at 35°C for 48 hr to determine the number of CFU/ml. Synergism and indifference were defined as a decrease of ≥2 $\log_{10}$ and <2 $\log_{10}$ CFU/ml with respect to the most active drug, and antagonism was defined as an increase of ≥2 $\log_{10}$ CFU/ml with respect to the least active drug.[41,42]

4.5.3 | Molecular dynamics simulation studies

To understand molecular level interactions between OAEE–AmB and OAEE–FLU, molecular simulation studies were carried out using the Desmond Molecular Dynamics system (Version 2.4; D. E. Shaw Research, New York, NY, 2010). A Maestro module 2D sketcher in Schrodinger software was used to draw structures of OAEE, AmB, and FLU and the structure refinements were done by ligand preparation (Ligprep module) module. Energy minimization of complexes of OAEE with AmB and FLU was performed using Macromodel module. The energy minimized complexes were immersed in the SPC water system in an orthorhombic box in system builder panel of Desmond. The system was relaxed before MDS using the default relaxation protocol. NPT ensemble was used at 300 K and the simulation was run for 10 ns. Different molecular interactions, as well as their stability over a 10-ns period, were studied from stored trajectories by calculating the parameters such as RMSD and RMSF.

4.5.4 | Atomic force microscopy

OAEE and its combination induced morphological alteration were evaluated using AFM. Briefly, an aliquot of *C. albicans* SP306 cell suspension with a cell density of 1×10^5 CFU/ml was introduced in a six-well plate (Hi-Media). The concentrations equivalent to OAEE (31.25 µg/ml), FLU (64 µg/ml), and AmB (1 µg/ml) were added separately and in combination (OAEE+FLU and OAEE+AmB) to the well. PS-treated cells served as a control. A sterile round glass cover slide was placed in each well, and the plate was incubated for 6 hr at 35°C. Later, the suspension from each well was carefully aspirated and the cover slides were washed twice with PS solution. The cover slides were then air-dried and fixed using a double-sided tape to the microscope holder. AFM (MFP-3D-BIO version-15.112, Asylum Research, Santa Barbara) was operated in tapping mode using a BL-AC40 TS (BioLever Mini); small nitride cantilever silicon tip f = 110 kHz and k = 0.09 N/m (Oxford Instruments, UK). Images were processed and roughness analysis expressed as RMS (i.e., the standard deviation of the distribution of heights over a 20 × 20-µm^2 imaged area) was calculated using Igor Pro software (WaveMetrics, Inc).[43]

4.6 | Activity of OAEE and its combinations on preformed *C. tropicalis* biofilm

4.6.1 | Minimal biofilm eradication concentration (MBEC)

An in vitro 96-well static microplate model was used to prepare preformed biofilms.[44] Briefly, 100 µl of fresh *C. tropicalis* suspension (1×10^6 CFU/ml) prepared in RPMI 1640 medium was introduced in each well of sterile, polystyrene, flat-bottomed 96-well plates (Hi-Media). Plates were kept stationary and incubated at 35°C for 24 hr to facilitating adherence. After 24 hr, the medium was carefully aspirated and nonadherent cells were removed by washing twice with sterile PS solution. Each well was replenished with 100 µl of fresh RPMI 1640 medium consisting of a range of test concentrations of FLU (8–1,024 µg/ml), AmB (1–128 µg/ml), and OAEE (15.625–2,000 µg/ml), separately. Plates were sealed using parafilm and incubated for 24 hr at 35°C. Post incubation, plates were washed twice with PS solution and incubated with 100 µl of XTT-menadione solution (1 µM prepared in 10-mM menadione–acetone solution) in the dark at 35°C for 2 hr. An aliquot of 90-µl solution from each well was transferred to a fresh 96-well plate and the absorbance was recorded at 492 nm.[45] The concentration producing a 50% reduction in XTT readings, as compared to the drug-free control, was marked as MIC_{50}.

4.6.2 | Checkerboard assay

A 2D (8 × 8) checkerboard microdilution method was used to determine the interaction of OAEE in combination with antifungal drugs (FLU and AmB) on prebiofilm. The choice of an appropriate range of drug concentration was based on MIC findings of individual antifungal agent. Briefly, 50 µl of two-fold OAEE concentration ranges were added vertically (A–H) and 50 µl of two-fold FLU or AmB dilutions were added horizontally (1–8) to the preformed biofilms in a 96-well plate. The interaction was quantified using XTT–menadione reduction solution. FICI was calculated and data were interpreted using the LA model.

4.6.3 | Atomic force microscopy

Flat sterile medical-grade silicone disks, with a total surface area of 314.159 mm^2, were placed in a 12-well, flat-bottom polystyrene plate (Hi-Media). A *C. tropicalis* M206 cell suspension (3 ml) containing 1×10^6 CFU/ml was pipetted into each well and incubated at 35°C for 24 hr. Disks were washed thrice with 5 ml of PS solution transferred to another 12-well microtiter plate containing 3 ml of test concentration; OAEE (125 µg/ml), FLU (128 µg/ml), and AmB (2 µg/ml) and their combinations, separately. The disks were incubated for 24 hr at 35°C. Post incubation, the disks were washed and dried at room

temperature for 1 hr. AFM analysis was conducted, as mentioned earlier. PS-treated disks served as a control.

4.7 | Cytotoxicity studies

In vitro cytotoxicity of OAEE was evaluated against HEK 293 and Hep2G using the sulforhodamine B (SRB) assay method. The concentrations ranging from 10 to 80 μg/ml were tested and compared with a cytotoxic doxorubicin formulation (adriamycin).[32] Growth inhibition (GI_{50}); the concentration resulting in a 50% reduction in the net protein increase (as measured by SRB staining) in control cells during the drug incubation, and LC_{50}; the concentration resulting in a 50% reduction in the measured protein at the end of the treatment as compared to that at the beginning, were calculated as per protocol described by Kalhapure et al.[46]

4.8 | Statistical analysis

Graphs were plotted using GraphPad Prism 6 (GraphPad Inc., San Diego, CA). Statistical analysis was performed using one-way analysis of variance, followed by post-hoc Bonferroni multiple comparison tests with a significance level of $p < 0.05$.

ACKNOWLEDGMENTS

This study was financially supported by the Department of Science and Technology, India under the Inspire fellowship (IF 130868) received by Mrunal Patil. Authors are grateful to the SAIF, CRNTS, and the Department of Biosciences and Bioengineering, IIT, Mumbai, for providing microscopy analysis facility and expertise. The authors acknowledge the Advanced Center for Treatment Research and Education in Cancer (ACTREC), Mumbai, India for the SRB assay.

CONFLICT OF INTERESTS

The authors declare that there are no conflict of interests.

ORCID

Mrunal Patil http://orcid.org/0000-0002-5722-6567
Pradeep Vavia http://orcid.org/0000-0001-8568-7857

REFERENCES

[1] N. Ding, W. Zhang, G. Lv, Y. Li, *Arch. Pharm.* **2011**, *344*, 786.
[2] N. Liu, J. Tu, G. Dong, Y. Wang, C. Sheng, *J. Med. Chem.* **2018**, *61*, 5484.
[3] V. Nagappan, D. Boikov, J. A. Vazquez, *Antimicrob. Agents Chemother.* **2010**, *54*, 522.
[4] F. Zhao, H. H. Dong, Y. H. Wang, T. Y. Wang, Z. H. Yan, F. Yan, D. Z. Zhang, Y. Y. Cao, Y. S. Jin, *MedChemComm* **2017**, *8*, 1093.
[5] S. Wang, Y. Wang, W. Liu, N. Liu, Y. Zhang, G. Dong, Y. Liu, Z. Li, X. He, Z. Miao, J. Yao, J. Li, W. Zhang, C. Sheng, *ACS Med. Chem. Lett.* **2014**, *5*, 506.
[6] E. J. Helmerhorst, I. M. Reijnders, W. van't Hof, I. Simoons-Smit, E. C. I. Veerman, A. V. N. Amerongen, *Antimicrob. Agents Chemother.* **1999**, *43*, 702.
[7] A. C. Mesa-Arango, C. Rueda, E. Román, J. Quintin, M. C. Terrón, D. Luque, M. G. Netea, J. Pla, O. Zaragoza, *Antimicrob. Agents Chemother.* **2016**, *60*, 2326.
[8] C. Tsui, E. F. Kong, M. A. Jabra-Rizk, *Pathog. Dis.* **2016**, *74*, ftw018.
[9] N. Wiederhold, *Infect. Drug Resist.* **2017**, *10*, 249.
[10] C. Girmenia, *Expert Opin. Invest. Drugs* **2009**, *18*, 1279.
[11] K. B. Steinbuch, R. I. Benhamou, L. Levin, R. Stein, M. Fridman, *ACS Infect. Dis.* **2018**, *4*, 825.
[12] D. B. Vieira, A. M. Carmona-Ribeiro, *J. Antimicrob. Chemother.* **2006**, *58*, 760.
[13] T. Misawa, C. Goto, N. Shibata, M. Hirano, Y. Kikuchi, M. Naito, Y. Demizu, *MedChemComm* **2019**.
[14] M. R. Infante, L. Pérez, A. Pinazo, P. Clapés, M. C. Morán, M. Angelet, M. T. García, M. P. Vinardell, *C. R. Chim.* **2004**, *7*, 583.
[15] A. Pinazo, M. A. Manresa, A. M. Marques, M. Bustelo, M. J. Espuny, L. Pérez, *Adv. Colloid. Interface Sci.* **2016**, *228*, 17.
[16] J. A. Castillo, A. Pinazo, J. Carilla, M. R. Infante, M. A. Alsina, I. Haro, *Langmuir* **2004**, *20*, 3379.
[17] A. Singh, V. K. Tyagi, *Tenside, Surfactants, Deterg.* **2014**, *51*, 202.
[18] L. Pinheiro, C. Faustino, *Application and characterization of surfactants*, IntechOpen, London, UK **2017**, p. 207.
[19] M. E. Fait, H. P. S. da Costa, C. D. T. Freitas, L. Bakás, S. R. Morcelle, *Curr. Bioact. Compd.* **2019**, *15*, 351.
[20] A. C. Wilson, M. A. Us, H. Zhang, S. B. Glazer, Patent US 7,074,447 B2, 2016.
[21] B. J. B. Urgell, B.J. Seguer, Patent US 7,862,842 B2, 2012.
[22] L. Li, I. Vorobyov, T. W. Allen, *J. Phys. Chem. B* **2013**, *117*, 11906.
[23] C. T. Armstrong, P. E. Mason, J. L. R. Anderson, C. E. Dempsey, *Sci. Rep.* **2016**, *6*, 21759.
[24] K. Patel, M. Tyagi, J. Monpara, L. Vora, S. Gupta, P. Vavia, *J. Nanopart. Res.* **2014**, *16*, 2345.
[25] N. Schmidt, A. Mishra, G. H. Lai, G. C. L. Wong, *FEBS Lett.* **2010**, *584*, 1806.
[26] L. T. Nguyen, L. de Boer, S. A. J. Zaat, H. J. Vogel, *BBA, Biochim. Biophys. Acta, Biomembr.* **1808**, *2011*, 2297.
[27] A. P. Desbois, V. J. Smith, *Appl. Microbiol. Biotechnol.* **2010**, *85*, 1629.
[28] J. H. Paul, W. H. Jeffrey, *Can. J. Microbiol.* **1985**, *31*, 224.
[29] B. A. Arthington-Skaggs, H. Jradi, T. Desai, C. J. Morrison, *J. Clin. Microbiol.* **1999**, *37*, 3332.
[30] S. Shreaz, R. Bhatia, N. Khan, S. Muralidhar, S. F. Basir, N. Manzoor, L. A. Khan, *Fitoterapia* **2011**, *82*, 1012.
[31] C. Ghosh, V. Yadav, W. Younis, H. Mohammad, Y. A. Hegazy, M. N. Seleem, K. Sanyal, J. Haldar, *ACS Infect. Dis.* **2017**, *3*, 293.
[32] D. M. Dhumal, K. G. Akamanchi, *Int. J. Pharm.* **2018**, *541*, 48.
[33] D. L. Zuza-Alves, W. P. Silva-Rocha, G. M. Chaves, *Front. Microbiol.* **2017**, *8*, 1927.
[34] M. Cavalheiro, M. C. Teixeira, *Front. Med.* **2018**, *5*, 28.
[35] Clinical Laboratory Standards Institute, *NCCLS Document M27-A2*, 22, 2002, p. 1.
[36] S. K. Shrestha, M. Y. Fosso, S. Garneau-Tsodikova, *Sci. Rep.* **2015**, *5*, 17070.
[37] M. Elshikh, S. Ahmed, S. Funston, P. Dunlop, M. McGaw, R. Marchant, I. M. Banat, *Biotechnol. Lett.* **2016**, *38*, 1015.
[38] F. De Seta, M. Schmidt, B. Vu, M. Essmann, B. Larsen, *J. Antimicrob. Chemother.* **2008**, *63*, 325.
[39] S. Vaidyanathan, B. G. Orr, M. M. Banaszak Holl, *J. Phys. Chem. B* **2014**, *118*, 2112.
[40] A. Ahmad, M. Y. Wani, M. Patel, A. J. F. N. Sobral, A. G. Duse, F. M. Aqlan, A. S. Al-Bogami, *MedChemComm* **2017**, *8*, 2195.
[41] N. Guo, G. Ling, X. Liang, J. Jin, J. Fan, J. Qiu, Y. Song, N. Huang, X. Wu, X. Wang, X. Deng, X. Deng, L. Yu, *Mycoses* **2011**, 54.
[42] A. Ahmad, A. Khan, N. Manzoor, *Eur. J. Pharm. Sci.* **2013**, *48*, 80.
[43] P. C. Braga, D. Ricci, *Methods Mol. Biol.* **2011**, *736*, 401.
[44] Q. Yu, X. Ding, N. Xu, X. Cheng, K. Qian, B. Zhang, L. Xing, M. Li, *Int. J. Antimicrob. Agents* **2013**, *41*, 179.

[45] J. You, L. Du, J. B. King, B. E. Hall, R. H. Cichewicz, *ACS Chem. Biol.* **2013**, *8*, 840.
[46] R. S. Kalhapure, K. G. Akamanchi, *Int. J. Pharm.* **2012**, *425*, 9.

SUPPORTING INFORMATION

Additional supporting information may be found online in the Supporting Information section.

How to cite this article: Patil M, Wanjare S, Borse V, Srivastava R, Mehta P, Vavia P. Arginolipid: A membrane-active antifungal agent and its synergistic potential to combat drug resistance in clinical *Candida* isolates. *Arch Pharm Chem Life Sci*. 2019;e1900180.
https://doi.org/10.1002/ardp.201900180